J Shanghai Univ (Engl Ed), 2008, 12(2): 171–179
Digital Object Identifier(DOI): 10.1007/s 11741-008-0216-1

Numerical study on the propagation characteristics of forward smoldering in a cellulosic packed bed

JIA Bao-shan (贾宝山)[1,2], XIE Mao-zhao (解茂昭)[1], LIU Hong (刘 红)[1]
1. School of Energy and Power, Dalian University of Technology, Dalian 116024, P. R. China
2. College of Safety Science and Engineering, Liaoning Technical University, Fuxin 123000, P. R. China

Abstract Based on a three-step kinetic mechanism, a one-dimensional, time dependent, numerical model is presented for the smoldering propagation in a horizontally packed bed of cellulosic material. The kinetic processes include pyrolysis and oxidation degradation of fuel and oxidation of char. Heat transfer between solid and gas is taken into account, and the diffusion coefficient varies with the temperature. Radiative heat transfer is included by using the diffusion approximation. The effects of airflow velocity and oxygen concentration are simulated on the smoldering velocity and the averaged maximum temperature of smoldering fuel. The results indicate that the spread rate varies linearly with increasing airflow velocity, and the inlet air velocity has little effect on the maximum temperature. The evolutions of gas species and solid compositions are predicted. The effects of frequency factors (A_1, A_2 and A_3) are analyzed. Simulations show that the smoldering spread rate increases with increasing A_2 (fuel oxidation), but decreases with A_1 (fuel pyrolysis) and A_3 (char oxidation).

Keywords forward smoldering, inlet air velocity, smoldering velocity, pre-exponential factor.

1 Introduction

Smoldering is an important phenomenon that, due to its implications for fire and toxicity safety, continues to attract the attention of combustion community. Smoldering is a slow and flameless combustion process in a porous medium in which heat is released by oxidative reactions[1]. In general, smoldering combustion takes place at relatively low temperature and small propagation velocity. If the material is sufficiently porous, the smoldering wave can propagate through the interior of porous materials. The smoldering wave is propagated in the form of heat conduction and radiation from the reaction zone to the unreacted fuel. Air is transferred through the pores to the reaction front where a heterogeneous exothermic reaction occurs between the solid and the gas[2]. Therefore, smoldering combustion in porous beds is very complicated both chemically and thermo-physically, which involves complex processes related to fluid flow, surface chemical reaction, heat and mass transfer in a porous media. The interaction between these physical and chemical processes determines the final characteristics of the smoldering reaction. In addition, the fuel's physical properties, including void fraction, permeability to gas flow thermal conductivity, specific heat, *etc.*, are important in determining the combustion reaction characteristics[3]. External factors like insulation from the environment, inlet air velocity and the nature of the ignition source are also important factors affecting the smoldering reaction characteristics and its smoldering velocity.

Smoldering combustion is an important potential source of fire hazard. So smoldering is significant in fire safety because it produces a great amount of toxic gases, which can cause people to lose consciousness and inhibit their respiration in an environment in which smoldering is usually far less conspicuous than a flaming fire. Another danger of smoldering in terms of fire safety is that it can cause initiation of a flaming fire through the transition from smoldering. Once transition takes place, flaming combustion engulfs the whole material quickly. This has the potential of causing more damage than normal flaming combustion[4]. According to the statistics, fire cases resulting from smoldering have already taken the first place in the USA. Moreover, this phenomenon has a wide range of technological relevance, as in the control of fire spread in permeable solids and high-temperature synthesis of materials. Therefore, during the last few decades, smoldering study has been receiving increasing attention in many countries, resulting in a large quantity of research findings[1−6].

Smoldering combustion is generally classified into forward and reverse configurations. In forward smoldering, the reaction zone propagates in the same direction

Received Sept.5, 2006; Revised Mar.9, 2007
Project supported by the National Natural Science Foundation of China (Grant No.50476073)
Corresponding author JIA Bao-shan, PhD Candidate, Assoc. Prof., E-mail: jiabaoshan72918@sina.com

as the inlet airflow. In reverse smoldering, the fresh airflow enters the reaction zone from opposite direction of smoldering wave propagation. Forward smoldering is unsteady and moves at a higher rate, and can eventually transit to flaming combustion as increasing smoldering velocity due to increased inlet air velocity or oxygen concentration[7]. Reverse smoldering is characterized by a steady propagation velocity and cannot transit into flaming.

Smoldering combustion of porous materials has previously been studied numerically, analytically, and experimentally. Torero, *et al.*[8] conducted an experimental and numerical study of forward smoldering of polyurethane foam. Air was used as an oxidizer and was forced in the direction of smolder of smoldering propagation under conditions that produced approximately one-dimensional forward smoldering propagation. It provided further understanding of the mechanisms controlling forward smoldering and verification of theoretical models of the problem. Measurements of the temperature histories at several locations throughout the foam sample were used to infer characteristics of smoldering process and calculate smoldering velocity along the sample length as a function of inlet airflow velocity. It is found that, as the airflow velocity was increased, there was a transition in the smoldering characteristics from a smoldering process characterized by the propagation of a single exothermic oxidation reaction to one characterized by propagation of two reactions, an oxidative smoldering reaction preceded by an endothermic pyrolysis reaction. The transition from smoldering combustion to flaming was observed in some experiments at inlet airflow velocities greater than 1.5 cm/s.

Ohlemiller, *et al.*[9] experimentally compared the propagation characteristics of forward and reverse smoldering in packed beds. Two types of permeable fuels were examined, a cellulosic loose fill insulation (wood fibers) and a particular polymer material (polyisocyanurate). There were marked qualitative and quantitative differences in the two smoldering propagation modes. Reverse smoldering quickly reaches a steady propagation rate determined largely by heat transfer processes, while forward smoldering propagation is unsteady and moves at lower rate that appears limited by the stoicheometry of char oxidation. Both modes of propagation were ultimately limited by the rate of oxygen supply.

In comparison with other combustion processes, fewer fundamental studies have been done on smoldering combustion. In this paper, based on the previous research, the forward smoldering is numerically simulated in the horizontally packed bed of cellulosic materials. Distributions of temperature are presented at different smoldering time. Evolutions of solid compositions and gas species are numerically simulated at a certain location. The effects of inlet air velocity and pre-exponential factors are examined on the smoldering characteristics.

2 Kinetic mechanism

The smoldering processes are described in detail by a three-step model which accounts for fuel pyrolysis (endothermic), oxidative (exothermic) degradation of fuel and char oxidation (exothermic), namely,

(1) Endothermic pyrolysis

$\text{fuel} \rightarrow n_{\text{C},1}\text{char} + n_{\text{CO},1}\text{CO} + n_{\text{CO}_2,1}\text{CO}_2 + n_{\text{H}_2\text{O},1}\text{H}_2\text{O} - \Delta h_1$;

(2) Exothermic thermal oxidation

$\text{fuel} + n_{\text{O}_2,2}\text{O}_2 \rightarrow n_{\text{C},2}\text{char} + n_{\text{CO},2}\text{CO} + n_{\text{CO}_2,2}\text{CO}_2 + n_{\text{H}_2\text{O},2}\text{H}_2\text{O} + \Delta h_2$;

(3) Exothermic char oxidation

$\text{char} + n_{\text{O}_2,3}\text{O}_2 \rightarrow n_{\text{A},3}\text{ash} + n_{\text{CO},3}\text{CO} + n_{\text{CO}_2,3}\text{CO}_2 + n_{\text{H}_2\text{O},3}\text{H}_2\text{O} + \Delta h_3$,

where Δh_i is the enthalpy of the ith reaction (i=1, 2, 3), $n_{j,i}$ is the stoichiometric coefficient by mass fraction of the ith reaction, and the subscript j denotes char (C), carbon monoxide (CO), carbon dioxide (CO_2), vapor (H_2O) and solid ash (A) respectively. Stoichiometric coefficients of above reactions are presented in Table 1, taken from [10].

Table 1 Stoichiometric coefficient (mass fraction)

	Stoichiometric coefficient	Value
Pyrolysis	$n_{\text{C},1}$	0.46
	$n_{\text{CO},1}$	0.01
	$n_{\text{CO}_2,1}$	0.03
	$n_{\text{H}_2\text{O},1}$	0.50
Fuel oxidation	$n_{\text{O}_2,2}$	0.41
	$n_{\text{C},2}$	0.29
	$n_{\text{CO},2}$	0.08
	$n_{\text{CO}_2,2}$	0.24
	$n_{\text{H}_2\text{O},2}$	0.80
Char oxidation	$n_{\text{O}_2,3}$	1.65
	$n_{\text{A},3}$	0.05
	$n_{\text{CO},3}$	0.50
	$n_{\text{CO}_2,3}$	1.80
	$n_{\text{H}_2\text{O},3}$	0.30

According to Arrhenius' Law, reaction rates are given by[11]

$$r_1 = A_1 \exp(-E_1/RT_{\text{s}})\rho_{\text{F}}, \quad (1)$$

$$r_2 = A_2 \exp(-E_2/RT_{\text{s}})\rho_{\text{F}}\rho_{\text{O}_2}, \quad (2)$$

$$r_3 = A_3 \exp(-E_3/RT_{\text{s}})\rho_{\text{C}}\rho_{\text{O}_2}, \quad (3)$$

where r_i is the reaction rate of the ith reaction, A_i is the pre-exponential factor, E_i is the activation energy,

R is the universal gas constant, T_s is the temperature of solid phase, and the density ρ has subscripts denoting solid fuel (F), char (C) and oxygen (O_2), respectively.

The packed bed of cellulosic material (wood fibers) is 800 mm long (L), 60 mm high (h). Airflow is forced into the packed bed from the left side, and the hot gas exits from the right side. The smoldering propagation direction is the same as the inlet air direction, namely forward smoldering. The configuration of the packed bed of cellulosic material is shown in Fig.1.

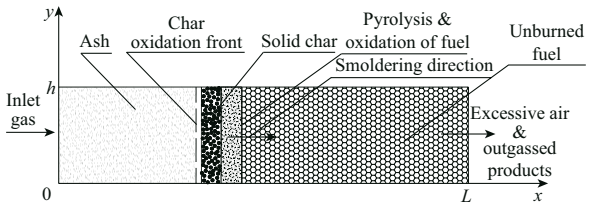

Fig.1 Schematic diagram of forward smoldering

3 Governing equations

In developing the governing transport equations, the following assumptions are introduced in order to simplify calculation:

(1) The fluid flow in porous medium is one-dimensional and laminar.

(2) Thermo-physical properties of the condensed phase (including foam, char and ash) and fluid are homogeneous and isotropic, and the chemical properties (including activation energy, pre-exponential frequency factor, enthalpy, *etc.*) remain constant during smoldering.

(3) The particles of cellulosic materials are spherical. The void between particles is saturated with fluid and the phases present in any small volume element are in thermal equilibrium.

(4) The porous matrix is rigid and incompressible, while volumetric change due to change of phase and chemical reaction is permitted.

(5) Heat only results from the oxidation reaction. There is no other source of volumetric heat in the packed bed.

(6) The ignition process in fuel bed is simulated by setting specified boundary and initial conditions.

(7) The gas mixture satisfies the state equation of ideal gas. The specific heats of all species are equal and constant, and Lewis number, Le, is 1.

(8) A decreasing density model is adopted for combustion mode of porous medium, and the volume of particles and porosity is unchanged during smoldering process[12].

The smoldering of porous medium is a process of two-phase (solid and gas) flow with chemical reactions. The numerical model consists of a set of conservation equations expressed as:

(1) Continuity equations of solid

$$\frac{\partial[(1-\varphi)\rho_F]}{\partial t} = A_s(-r_1 - r_2), \tag{4}$$

$$\frac{\partial[(1-\varphi)\rho_C]}{\partial t} = A_s(n_{C,1}r_1 + n_{C,2}r_2 - r_3), \tag{5}$$

$$\frac{\partial[(1-\varphi)\rho_A]}{\partial t} = A_s(n_{A,3}r_3), \tag{6}$$

where φ is the porosity of fuel packed bed, ρ_F, ρ_C and ρ_A the bulk density of fuel, char and ash respectively, and A_s a shaping factor of porous particles in packed bed, equal to the ratio of the surface area to the volume of particle, namely[13],

$$A_s = 6(1-\varphi)/d_p.$$

Here d_p is the diameter of spherical particle which is taken as the average diameter of fuel in this work.

(2) Continuity equations of gas

$$\frac{\partial\varphi\rho_g}{\partial t} + \frac{\partial\varphi\rho_g v}{\partial x} = A_s[(1-n_{C,1})r_1 + (1+n_{O_2,2}-n_{C,2})r_2 + (1+n_{O_2,3}-n_{A,3})r_3], \tag{7}$$

where ρ_g is the density of gas, and v the gas velocity through the porous fuel along the packed bed.

(3) Diffusion equations of gas species

$$\frac{\partial\varphi\rho_g Y_i}{\partial t} + \frac{\partial\varphi\rho_g v Y_i}{\partial x} = \Omega_i + \frac{\partial}{\partial x}\left(\varphi\rho_g D\frac{\partial Y_i}{\partial x}\right), \tag{8}$$

where $\Omega_i = A_s \sum_{j=1}^{3} \pm n_{i,j} r_j$ ($i = O_2$, CO, CO_2, H_2O), r_j is the reaction rate of the jth reaction ($j = 1, 2, 3$), the negative sign is for consumed gas species, and the positive sign for generated species, Y_i is the mass fraction of gaseous species.

Moreover, since transport of oxygen to the burn front depends critically on its ability to diffuse through the gas phase, it is important to include correct dependence of diffusivity on temperature[14]. The diffusion coefficient is expressed by[15]

$$D = 0.677 D_g \varphi^{1.18} (T_g/273)^{1.75},$$

where D_g is the unrestrained diffusion of the gas in a binary mixture, and T_g the temperature of the gas phase.

(4) Energy equation of solid phase

$$\frac{\partial}{\partial t}[(1-\varphi)(\rho_F C_F + \rho_C C_C + \rho_A C_A)T_s] = \frac{\partial}{\partial x}\left((1-\varphi)k_{eff}\frac{\partial T_s}{\partial x}\right) + A_s\sum_{i=1}^{3} r_i \Delta h_i + h_{s\text{-}g} A_s (T_g - T_s), \tag{9}$$

where C_F, C_C and C_A are the specific heat of fuel, char and ash respectively, T_s the temperature of solid phase, $h_{s\text{-}g}$ the gas-solid interface heat transfer coefficient, k_{eff} effective heat conductivity of porous medium and $k_{eff} = (1-\varphi)k_s + 16\delta d T_s^3/3$[16], k_s thermal conductivity of solid, δ the Stefan-Boltzmann constant, and d the pore diameter.

(5) Energy equation of gas phase

$$\frac{\partial}{\partial t}(\varphi\rho_g C_g T_g) + \frac{\partial}{\partial x}(\varphi\rho_g v C_g T_g) = \frac{\partial}{\partial x}\left(\varphi k_g \frac{\partial T_g}{\partial x}\right) + h_{s\text{-}g}A_s(T_s - T_g), \quad (10)$$

where C_g is the specific heat of gas, and k_g the thermal conductivity of gas.

Wakao, *et al.*[17] proposed a correlation for the coefficient of internal heat transfer between spheres and the fluid forced through it in packed bed. The convective heat transfer coefficient modeled as a function of Reynolds and Prandtl numbers is given by

$$Nu = \frac{h_{s\text{-}g}d_p}{k_g} = 2 + 1.1Re^{0.6}Pr^{1/3}.$$

This correlation can be used for smoldering combustion by setting $Re = 0$[18].

(6) Momentum equation

$$\frac{\partial}{\partial t}(\varphi\rho_g v) + \frac{\partial}{\partial x}(\varphi\rho_g v^2) = -\varphi\frac{\partial p}{\partial x} - C_1\mu_g v - C_2\mu_g v^2, \quad (11)$$

where μ_g is the dynamic viscosity coefficient, p the gas pressure, and C_1 and C_2 resistance coefficient for gas flow in porous media[19]. C_1 and C_2 are given by

$$C_1 = 150(1-\varphi)^2/(\varphi^3 d_p^2), \quad C_2 = 1.75(1-\varphi)/(\varphi^3 d_p).$$

(7) State equation of gas

$$p = \frac{\rho_g R T_g}{M_{mix}}, \quad (12)$$

where M_{mix} is the molecular weight of mixture gas and $M_{mix}^{-1} = \sum \frac{Y_i}{M_i}$ (i = O_2, CO, CO_2, N_2, H_2O), Y_i the mass fraction of gaseous species and $\sum Y_i = 1$, and M_i the molecular weight of the ith gaseous species.

As a whole, the governing equations contain nine parameters: ρ_g, Y_i, T_s, T_g, ρ_F, ρ_C, ρ_A, v, p.

There are nine independent equations, thus the problem is closed and can be solved.

4 Boundary and initial conditions

The computation model is shown in Fig.1. Airflow is forced into the fuel packed bed from left side at velocity of 0.49 cm/s. Hot gases including generated gaseous species exit from the right side. Smoldering propagation direction is also from the left to right through the packed bed, that is, forward smoldering.

4.1 Boundary conditions

(1) At the left boundary $x = 0$, parameters are specified by $T(0,t) = \begin{cases} 900\text{ K}, & t < 60\text{ s} \\ 300\text{ K}, & t \geqslant 60\text{ s} \end{cases}$, $p(0,t) = 1.01\times10^5$ Pa, $v(0,t) = 0.49$ cm/s, $\rho_g = 1.164$ kg/m^3, $\nabla Y_{O_2} = 0$, $\nabla\rho_j = 0\,(j$ = F, C, A). The condition of temperature is used to simulate the initiation process.

(2) At the right boundary $x = L$, the hot gas exit and the gradients of parameters are assumed to be zero: $\nabla T_s = 0$; $\nabla T_g = 0$; $\nabla P = 0$; $\nabla Y_i = 0$ (i = CO, CO_2, H_2O, O_2); $\nabla\rho_j = 0$ (j = F, C, A).

(3) At the bottom and top surfaces, the walls are assumed to be thermal insulation.

4.2 Initial boundary

At $t = 0$, the entire fuel bed is not reacted, all parameters including temperature, gas species, solid density are constant: $T_{s0} = 300$ K, $T_{g0} = 300$ K, $Y_{O_2,0} = 0.23$, $Y_{CO,0} = 0$, $Y_{CO_2,0} = 0.00032$, $Y_{H_2O,0} = 0.002$, $p_0 = 1.01\times10^5$ Pa, $\rho_{F0} = 34$ kg/m^3, $\rho_{C0} = 0$, $\rho_{A0} = 0$, $\rho_{g0} = 1.164$ kg/m^3, $v_{inelt} = 0.49$ cm/s, where the subscript zero denotes the initial value, and v_{inlet} the inlet gas velocity incoming the packed bed from the left boundary. The ignition temperature is fixed at 900 K for a time period of 60 s and the smoldering wave starts propagation forward along the packed bed.

5 Results and discussion

As shown in Fig.2, the packed bed is divided into 960 grids to perform calculations. The governing equations, boundary and initial conditions are rearranged and discretized in space by using finite element techniques. For this problem, COMSOL Multiphysics3.2 is used in conjunction with Matlab. COMSOL Multiphysics is a modeling package for simulation of any physical process you can describe with partial differential equations (PDEs). The properties of fuel are chosen from [9–11] as presented in Table 2.

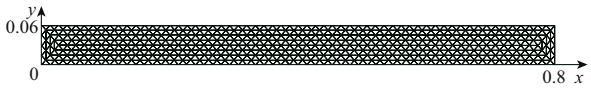

Fig.2 Computational mesh

5.1 Profiles of smoldering temperature

Profiles of solid temperature distribution at different time are plotted in Fig.3 along the packed bed (v_{inlet} = 0.49 cm/s). The average maximum temperature is 687.62 K and the average smoldering velocity is 0.028 cm/s. As shown in Fig.3, the packed bed of cellulosic materials can be divided into three zones:

Table 2 Characteristic parameters of fuel

Property	Value	Unit
E_1	220	kJ/mol
E_2	160	kJ/mol
E_3	160	kJ/mol
A_1	2.0×10^{17}	/s
A_2	2.5×10^{12}	$m^3/(kg{\cdot}s)$
A_3	5.7×10^{9}	$m^3/(kg{\cdot}s)$
C_F	2.3	kJ/(kg·K)
C_C	1.1	kJ/(kg·K)
C_A	1.1	kJ/(kg·K)
C_g	1.1	kJ/(kg·K)
k_s	0.063	W/(m·K)
φ	95	%
μ_g	3×10^{-5}	kg/(m·s)
Δh_1	−570	kJ/kg
Δh_2	5709	kJ/kg
Δh_3	25050	kJ/kg
D_g	2×10^{-5}	m^2/s
d_p	4×10^{-4}	m
d	1×10^{-4}	m
ρ_{ref}	1.164	kg/m^3
k_g	0.0258	W/(m·K)

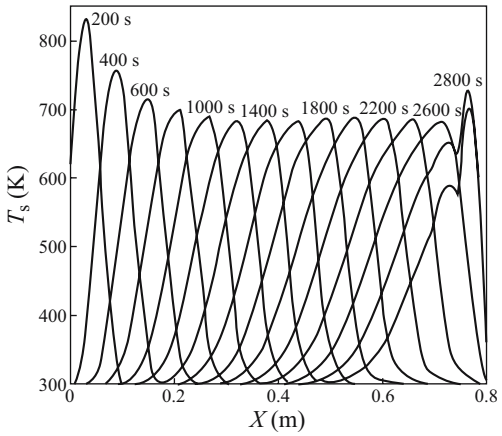

Fig.3 Profiles of solid temperature

Zone I: initial zone ($0 < X < 0.14$ m). This zone is near the igniter whose length mainly depends on the inlet gas velocity and ignition temperature at the boundary. The smoldering velocity is faster than 0.0289 cm/s in this case. Thus, smoldering in zone I is not representative of the type of smoldering studied here, and only limited data from this zone are presented.

Zone II: stable smoldering zone (0.14 m $\leqslant X \leqslant$ 0.7 m). This region lies in the middle of the packed bed. Since there is no interference in this zone from the external environment, the smoldering propagation of fuel is relatively stable, and the smoldering velocity is 0.028 cm/s. The maximum temperature is 687.62 K. The smoldering propagation in zone II is the most representative of forced flow forward smoldering, at least from the point of view of modeling, since external effects are limited.

Zone III: end zone (0.7 m $< X < 0.8$ m). This zone is located at the end of the packed bed that is 100 mm long from the exiting boundary, so smoldering is affected by the external environment. The smoldering in zone III is unstable but is of particular interest for observing the effect of external ambient.

During smoldering, heat transfer takes place between the solid and gas phases. So at a certain location of the smoldering wave front, temperature of solid is not the same as that of the gas. The temperature difference between the two phases is presented in Fig.4 at 1200 s, 1600 s and 2000 s. First, ahead of the front, airflow is heated by the high-temperature solid through radiation and convection, so the temperature of solid is higher than gas. When the airflow enters the reaction front, the temperature of solid and gas will become the same with the peak value of 687.62 K. When the hot air flows out the reaction front, its temperature is higher than the solid due to the different conductivity between solid and gas. Finally, temperatures of solid and gas will decrease to the ambient temperature (300 K).

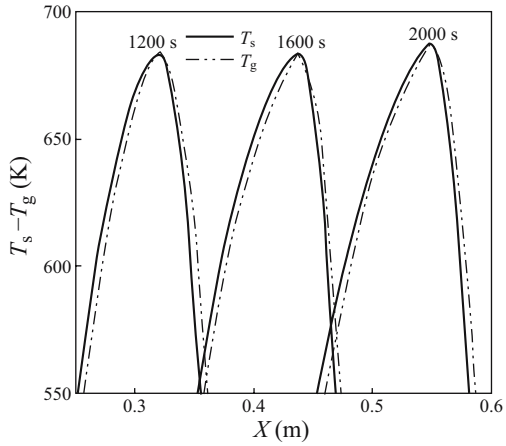

Fig.4 Distribution of solid-gas temperature

5.2 Evolution of gas species

Fig.5 presents the evolution of mass fraction of gas species when the smoldering front is located at 0.405 m (v_{inlet} = 0.49 cm/s). The mass fraction of O_2 (Y_{O_2}) decreases from 0.23 to 0.0484 due to the oxidatative reactions of fuel and char. When smoldering front propagates through the location 0.405 m, mass fraction of O_2 gradually increases to the original value 0.23 due to the provision of inlet airflow. Since the carbon monoxide (CO) is a gaseous product generated from the three reactions, the mass fraction of CO (Y_{CO}) gradually increases from 0 to 0.0912. Soon it decreases gradually to

0 with the movement forward of smoldering front due to the dilution of inlet airflow. In the same way, Y_{CO_2} first increases from 0.00032 to 0.183 and then decreases to 0.00032. The quantity of H_2O produced from reactions is the most, and the maximum value of Y_{H_2O} is 0.263. Moreover, the gas species of H_2O, CO and CO_2 are generated ahead of the consumption of oxygen because the first reaction is the pyrolysis of fuel without oxygen participation.

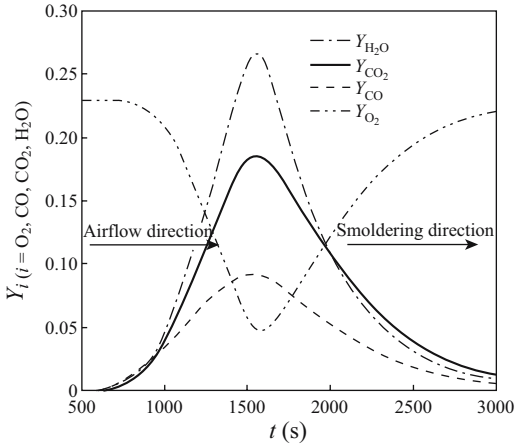

Fig.5 The evolution of gas species (X = 0.405 m)

5.3 Evolution of solid compositions

In Fig.6, the evolutions of solid compositions including fuel, char and ash are presented along the fuel packed bed at X = 0.405 m for the base case. The packed bed can be obviously divided into four zones: unreacted zone (X>0.445 m), fuel pyrolysis and oxidation zone (0.369 m<X<0.445 m), char oxidation zone (0.295 m<X<0.369 m) and burned-out zone (X<0.295 m).

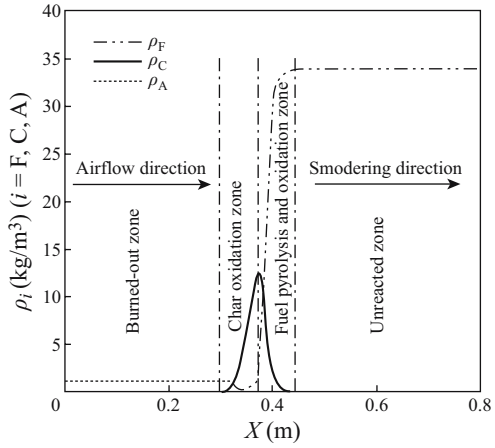

Fig.6 The evolution of solid compositions (X = 0.405 m)

In the unreacted zone, the density of fuel is its original value 34 kg/m^3. In the zone of fuel prolysis and oxidation, the pyrolysis and oxidation reactions of fuel occur simultaneously. Some char is transformed during the two reactions and its density is various from zero to 12.512 kg/m^3. The fuel density decreases from 34 kg/m^3 to 5.471 kg/m^3 due to consumption. In addition, with the generation of char, a little ash is generated and its density increases from zero to 0.119 kg/m^3. The results indicate that the quantity of char generated is much greater than that of oxidized, so the density of char is gradually accelerated to its peak value in this zone.

In char oxidation zone, char is further oxidized into ash whose density increases from 0.119 kg/m^3 to 1.093 kg/m^3, and the density of char decreases from 12.512 kg/m^3 to zero. There is some fuel left to further pyrolysis and oxidation, so some char is also generated. However, the quantity of char oxidized in this zone is much greater than that of generated.

Finally, in the burned-out zone, there is only ash left as residual solid products that do not react any more. The density of ash is a constant 1.093 kg/m^3.

At the inlet air velocity of 0.49 cm/s, the pyrolysis front of fuel moves to a position of 0.076 m ahead of the char oxidation front. The distance between the two fronts will be shortened with increasing inlet air velocity. The variation trend results from the greatly accelerating char oxidation owing to abundant oxygen supply. Moreover, in char oxidation zone, there is a little unburned fuel left whose density varies from 5.471 kg/m^3 to zero. It is indicated that the three reactions (pyrolysis, fuel oxidation and char oxidation) take place simultaneously during the smoldering wave propagation.

5.4 Effect of oxygen concentration

The effects of mass fraction of oxygen (Y_{O_2}) on the smoldering velocity and maximum temperature are presented in Fig.7. With an inlet air velocity of 0.49 cm/s, different values of Y_{O_2} from 0.15 to 0.9 are used to simulate the smoldering propagation. The results indicate that smoldering velocity increases by a factor of

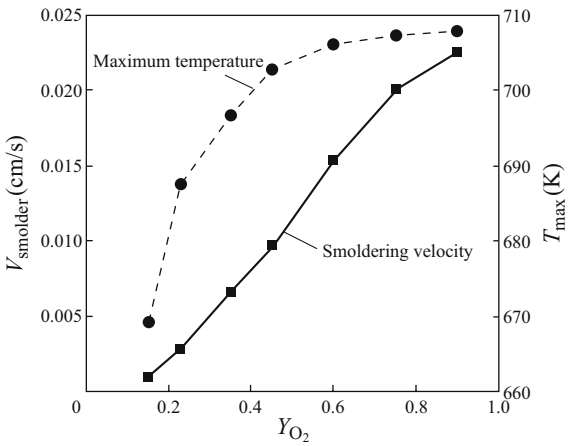

Fig.7 Relationship between smoldering and Y_{O_2}

25.6 cm/s from 0.088 cm/s to 2.25 cm/s with increasing Y_{O_2} by a factor of 6 from 0.15 to 0.9. The relation between the two parameters appears roughly linear. It can be seen that oxygen concentration of inlet airflow has important effect on smoldering propagation because increasing oxygen concentration can enhance fuel oxidation process and, in turn, increase the smoldering propagation velocity.

The maximum temperature (T_{max}) of solid fuel is also presented in Fig.7. The results show an increase in temperature from 669.19 K to 707.94 K with increasing Y_{O_2} from 0.15 to 0.9. But when Y_{O_2} is greater than 0.6, the increase in the maximum temperature is very small (from 706.18 K to 707.94 K) because, in this case, the fuel is completely burned and oxygen is superfluous. The increased smoldering velocity is helpful to accelerate heat transfer.

5.5 Effect of inlet air velocity

The increased velocity of inlet airflow leads to an increased oxygen supply. For the smoldering process of solid fuel at the stoichometric condition, the ratio of the gaseous oxidant flux (Q_{Air}) to consumed solid flux (Q_{Fuel}) entering the reaction zone is nearly a constant[9], namely,

$$\frac{Q_{Air}}{Q_{Fuel}} = \frac{\varphi\rho_g V_{inlet}}{(1-\varphi)\rho_F V_{smolder}} \approx \text{const},$$

where φ is the void fraction in the packed bed of fuel, ρ_g the density of inlet airflow, V_{inlet} the velocity of inlet airflow, ρ_F the true density of the solid fuel, and $V_{smolder}$ the smoldering velocity of fuel. The air/fuel ratio for cellulosic materials is about 5.9.

The effect of inlet air velocity on the smoldering velocity is presented in Fig.8. When the inlet air velocity varies from 0.15 cm/s to 0.49 cm/s, the smoldering velocity linearly increases from 0.0118 cm/s to 0.0286 cm/s. The computational results agree very well with the experimental data of Ohlemiller, *et al.*[9].

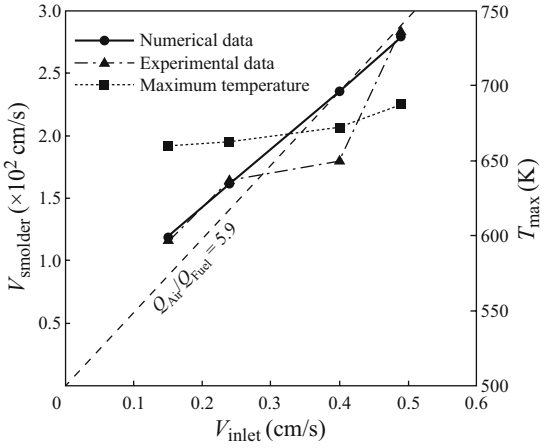

Fig.8 Relationship between smoldering and inlet velocities

The dashed line in Fig.8 corresponds to a constant air/fuel ratio ($Q_{Air}/Q_{Fuel} = 5.9$).

Moreover, the effect of inlet air velocity on the maximum temperature (T_{max}) of solid is also presented in Fig.8. The average maximum temperature of solid increases from 659.93 K to 687.62 K as increasing the inlet air velocity from 0.15 cm/s to 0.49 cm/s. It appears that the maximum temperature increases less than 30 K while inlet air velocity is increased by a factor of 3.3. Therefore, the inlet air velocity has little effect on the maximum temperature.

5.6 Effect of pre-exponential factor

Smoldering is a self-maintained combustion process. The heat source driving the smoldering propagation is the two exothermic reactions, *i.e.*, fuel and char oxidation. To investigate the effects of reaction rates on the smoldering combustion, simulations have been performed by varying separately A_1 (fuel pyrolysis), A_2 (fuel oxidation) and A_3 (char oxidation). Simulated results are summarized in Figs.9, 10 and 11, respectively.

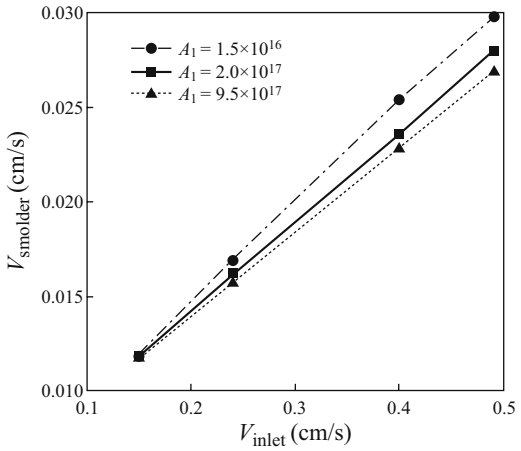

Fig.9 Effect of A_1 on the smoldering velocity

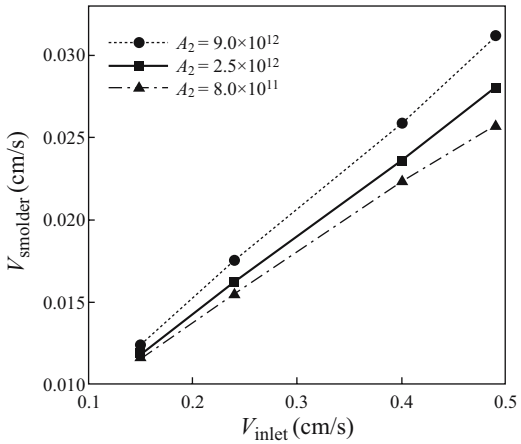

Fig.10 Effect of A_2 on the smoldering velocity

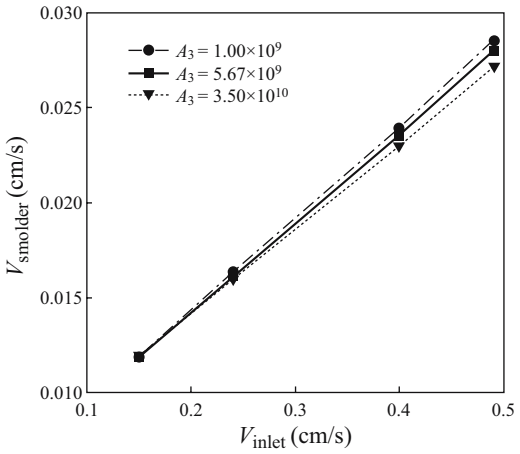

Fig.11 Effect of A_3 on the smoldering velocity

(1) Effect of pre-exponential frequency factor of fuel pyrolysis (A_1)

First, the values of A_2 and A_3 are specified as constants, 2.5×10^{12} and 5.67×10^9, respectively. The different values of A_1 (from 1.5×10^{16} to 9.5×10^{17}) are used to examine its role. As Fig.9 shows, smoldering velocity increases with decreasing A_1. The reason is that a smaller A_1 can slow down the reaction of fuel pyrolysis that will require less heat for pyrolyzing. Consequently, the temperature in the reaction zone is raised resulting in an increase in the smoldering velocity.

In opposition, the smoldering propagation will be restrained by increasing the value of A_1.

(2) Effect of pre-exponential frequency factor of fuel oxidation (A_2)

Fig.10 shows that increasing A_2 from 8×10^{11} to 9×10^{12} will lead to an increase in the smoldering velocity from 0.257 cm/s to 0.312 cm/s for the basic case ($V_{\text{inlet}} = 0.49$ cm/s). A larger A_2 means the acceleration of fuel oxidation and gives out more heat. So the smoldering velocity is increased.

(3) Effect of pre-exponential frequency factor of char oxidation (A_3)

In Fig.11, the effect of A_3 on smoldering velocity is presented for different values from 1.0×10^9 to 3.5×10^{10}. It appears that A_3 has little effect on the smoldering velocity. However, as A_3 is increased, the smoldering velocity slightly decreases. The reason is that increasing char oxidation will consume more oxygen and reduce the oxygen supply for fuel oxidation. However, fuel oxidation is the dominative reaction driving the smoldering process. The simulated results of Leach[16] for polyurethane foam show that the heat release of fuel oxidation is about 20 times as much as that of char oxidation. Thus A_3 has little effect on the smoldering propagation.

In addition, Figs.9, 10 and 11 give the simulated results at different velocities of inlet air. They show that changing the pre-exponential frequency factor has little effect on the smoldering velocity at a low inlet air velocity, *e.g.*, 0.15 cm/s or 0.24 cm/s, but has clear effect at higher velocities, *e.g.*, 0.4 cm/s and 0.49 cm/s. It appears that smoldering is oxygen limited at low inlet air velocities and kinetically limited at higher velocities. Simultaneously, during the smoldering process, the most important process driving the smoldering propagation is fuel oxidation, the second is fuel pyrolysis, and the least is char oxidation. When the A_3 is zero (without char oxidation), the smoldering process can still continue to propagate. So char oxidation plays only a slight role in driving the smoldering propagation.

6 Conclusions

(1) Based on a three-step kinetic mechanism, a one-dimensional, unsteady, model of forward smoldering in a porous medium has been developed.

(2) The oxygen concentration is important in the smoldering propagation. With increasing mass fraction of oxygen, the smoldering velocity observably increases. However, the maximum temperature has a limited increase which becomes small when Y_{O_2} is greater than 0.6.

(3) Simulated results indicate that the smoldering velocity increases linearly with increasing inlet air velocity, and the increasing trend is in accordance with the line of $Q_{\text{Air}}/Q_{\text{Fuel}} = 5.9$. The inlet air velocity has little effect on the maximum temperature of solid.

(4) The evolutions of solid compositions indicate that the three reactions are taking place at the same time. And it is more legible for us to understand the three-step kinetic mechanisms.

(5) Simulations have been conducted by varying separately A_1, A_2 and A_3 to examine the effects of reaction rates on the smoldering combustion. The results indicate that increasing A_2 (fuel oxidation) can accelerate the smoldering velocity, while increasing A_1 (fuel pyrolysis) and A_2 (char oxidation) will decrease the smoldering velocity.

(6) To drive a smoldering process, the most important reaction is fuel oxidation, the next is fuel pyrolysis, and the least important is char oxidation. The smoldering is oxygen limited at lower inlet air velocities and kinetically limited at higher velocities.

References

[1] Aldushin A P, Bayliss A, Matkowsky B J. On the transition from smoldering to flaming [J]. *Combustion and Flame*, 2006, **145**(4): 579–606.

[2] Bar-Ilan A, Rein G, Walther D, Fernandez-Pello A C, Torero J L, Urban D L. The effect of buoyancy on opposed smoldering [J]. *Combustion Science and Technology*, 2004, **176**(12): 2027–2055.

[3] Rein G, Lautenberger C, Fernandez-Pello A C, Torero J L, Urban D L. Application of genetic algorithms and thermogravimetry to determine the kinetics of polyurethane foam in smoldering combustion [J]. *Combustion and Flame*, 2006, **146**(1-2): 95–108.

[4] Chao C Y H, Wang J H. Transition from smoldering to flaming combustion of horizaontally oriented flexible polyurethane foam with natural convection [J]. *Combustion and Flame*, 2001, **127**(4): 2252–2264.

[5] Wang J H, Chao C Y H, Kong W J. Forced forward smoldering propagation in horizontally oriented flexible polyurethane foam [J]. *Journal of Fire Sciences*, 2002, **20**(2): 113–131.

[6] Xie M Z, Liang X H. Numerical simulation of combustion and ignition-quenching behavior of a carbon packed bed [J]. *Combustion Science and Technology*, 1997, **125**(1-6): 1–24.

[7] Wang J H, Chao C Y H, Kong W J. Experimental study and asymptotic analysis of horizontally forced forward smoldering combustion [J]. *Combustion and Flame*, 2003, **135**(4): 405–419.

[8] Torero J L, Fernandez-Pello A C. Forward smolder of polyurethane foam in a forced air flow [J]. *Combustion and Flame*, 1996, **106**(1-2): 89–109.

[9] Ohlemiller T J, Lucca D A. An experimental comparison of forward and reverse smolder propagation in permeable fuel beds [J]. *Combustion and Flame*, 1983, **54**(1-3): 131–147.

[10] Kashiwagi T, Nambu H. Global kinetic constants for thermal oxidative degradation of a cellulosic paper [J]. *Combustion and Flame*, 1992, **88**(3-4): 345–368.

[11] Di Blasi C. Mechnisms of two-dimensional smoldering propagation through packed beds [J]. *Combustion Science and Technology*, 1995, **106**(4-6): 103–124.

[12] Young B C, Smith I W. The combustion of loy young brown coal char [J]. *Combustion and Flame*, 1989, **76**(1): 29–35.

[13] Xie Mao-zhao, Reinelt D. Computational investigation on combustion of a carbon packed bed in stagnation flow field [J]. *Journal of Dalian University of Technology*, 1995, **35**(3): 362–366 (in Chinese).

[14] Sekely J, Evans J, Sohn H. *Gas-Solid Reactions* [M]. New York: Academic Press, 1976.

[15] Saidi M S, Mhaisekar A, Subbiah M. Effects of thermo-physical and flow parameters on the static and dynamic burning of a cigarette [J]. *Combustion Theory and Modelling*, 2006, **10**(6): 939–960.

[16] Leach S V, Rein G, Ellzey J L, Ezekoye O A, Torero J L. Kinetic and fuel property effects on forward smolder combustion [J]. *Combustion and Flame*, 2000, **120**(3): 346–358.

[17] Wakao N, Kaguei S. *Heat and Mass Transfer in Packed Beds* [M]. New York: Gordon and Breach Science Publisher, 1982.

[18] Rostami A, Murthy J, Hajaligol M. Modeling of a smoldering cigarette [J]. *Journal of Analytical and Applied Pyrolysis*, 2003, **66**(1-2): 281–301.

[19] Guo X P, Xie M Z. A mathematical model for smoldering propagation in a two-dimensional packed bed [J]. *Journal of Combustion Science and Technology*, 1995, **1**(1): 86–93.

(Editor CHEN Ai-ping)